British Journal of Pharmacology

DOI:10.1111/j.1476-5381.2011.01581.x
www.brjpharmacol.org

RESEARCH PAPER

Recombinant viral protein promotes apoptosis and suppresses invasion of ovarian adenocarcinoma cells by targeting α5β1 integrin to down-regulate Akt and MMP-2

Correspondence
Dr Shu-Mei Liang, Agricultural Biotechnology Research Center, Academia Sinica, Taipei 115, Taiwan. E-mail: smyang@gate.sinica.edu.tw; or
Dr Chi-Ming Liang, Genomics Research Center, Academia Sinica, Taipei, 115, Taiwan. E-mail: cmliang@gate.sinica.edu.tw

Keywords
chemotherapeutic agent; apoptosis; metastasis; integrin; ovarian cancer

Received
26 Jane 2011
Revised
9 June 2011
Accepted
17 June 2011

Jei-Ming Peng[1,2,3], Yee-Hsiung Chen[1,2], Shao-Wen Hung[4], Ching-Feng Chiu[4,5], Ming-Yi Ho[3], Yi-Jen Lee[6], Tsung-Ching Lai[3], Michael Hsiao[3], Chi-Ming Liang[2,3] and Shu-Mei Liang[4,5]

[1]*Institute of Biochemical Sciences, College of Life Science, National Taiwan University, Taipei, Taiwan,* [2]*Institutes of Biological Chemistry, Academia Sinica, Taipei, Taiwan,* [3]*Genomics Research Center, Academia Sinica, Taipei, Taiwan,* [4]*Agricultural Biotechnology Research Center, Academia Sinica, Taipei, Taiwan,* [5]*Institute of Biotechnology, National Cheng Kung University, Tainan, Taiwan, and* [6]*Department of Obstetrics and Gynecology, Tri-Service General Hospital, Taipei, Taiwan*

BACKGROUND AND PURPOSE

As prognosis for patients with metastatic ovarian cancer is generally poor, advances in treatment are needed. Here, we studied the mechanism of action of a recombinant viral capsid protein (rVP1) and explored its effect against ovarian tumour growth and metastasis *in vivo*.

EXPERIMENTAL APPROACH

The human ovarian cancer cell line SKOV3 and BALB/cAnN-Foxn1 female nude mice were used. Effects of rVP1 on the viability, invasive ability, matrix metalloproteinase (MMP)-2 activity and cancer cell proliferation and metastasis were determined by cell proliferation assay, Matrigel invasion assay, gelatin zymographic analysis, as well as bioluminescence imaging and immunohistological analysis in xenograft mouse models respectively. Levels of total and phosphorylated focal adhesion kinase (FAK), PKB/Akt, phosphatase and tensin homologue (PTEN) and glycogen synthase kinase-3β (GSK-3β) were detected by Western blotting.

KEY RESULTS

rVP1 promoted apoptosis and decreased invasion of human ovarian cancer cells. This effect of rVP1 was accompanied by activation of PTEN and GSK-3β as well as down-regulation of FAK, Akt and MMP-2. Anti-integrin antibodies or overexpression of constitutively active Akt reversed the cellular effects of rVP1. Orthotopic and intraperitoneal xenograft mouse models demonstrated that rVP1 attenuated survival and metastasis of human ovarian cancer SKOV3 cell line *in vivo* through selective regulation of Akt and GSK-3β activity as shown by bioluminescence imaging of mice and immunohistochemical analysis.

CONCLUSION AND IMPLICATIONS

These results indicate that negative regulation of Akt signalling and MMP-2 by rVP1 may have the potential to suppress ovarian tumour growth and metastasis *in vivo*.

Abbreviations

FAK, focal adhesion kinase; FMDV, foot-and-mouth disease virus; GFP, green fluorescent protein; GSK-3β, glycogen synthase kinase-3β; H&E, hematoxylin and eosin; PTEN, phosphatase and tensin homologue; rVP1, recombinant viral capsid protein

© 2011 The Authors
British Journal of Pharmacology © 2011 The British Pharmacological Society

Introduction

Ovarian cancer is the leading cause of death associated with gynaecological malignancies (Jemal *et al.*, 2009) and most ovarian cancers are derived from the epithelial cells that cover the surface of the ovary (Auersperg *et al.*, 2001; Cannistra, 2004). After an ovarian epithelial cell undergoes transformation, the cancer cell usually detaches from the surface basement membrane and metastasizes rapidly throughout the peritoneal cavity. Consequently, ovarian cancer is frequently discovered after tumour cells have already spread widely, resulting in peritoneal dissemination and massive accumulation of ascitic fluid. Although macronodular tumours in patients with epithelial ovarian cancer may be removed surgically, micronodular and floating tumour colonies are extremely difficult to remove completely by surgical means. Thus, chemotherapy has generally been adopted after surgery. Unfortunately, even after chemotherapy using the best drugs currently available such as paclitaxel, *cis*-platinum analogues and doxorubicin (Stearns and Wang, 1992; Rowinsky and Donehower, 1995; Klauber *et al.*, 1997; Lau *et al.*, 1999; Mano *et al.*, 2007), more than half of patients relapse and eventually die from the cancer (Cannistra, 2004). Therefore, development of more effective treatments for inhibition, not only of proliferation, but also of metastasis of advanced ovarian cancer cells is urgently needed.

Cancer deaths predominantly result from the formation of metastases (Kopfstein and Christofori, 2006). The fundamental component affecting normal and cancer cell motility is focal adhesion. Focal adhesion kinase (FAK) is a key mediator linking integrins to downstream signalling pathways involved in focal adhesion, the suppression of apoptosis, and the promotion of cell survival through activation of PKB/Akt and inactivation of glycogen synthase kinase-3β (GSK-3β) (Delcommenne *et al.*, 1998; Dedhar, 1999). Inactivation of GSK-3β by phosphorylation at Ser^{9} inhibits the phosphatase and tensin homologue (PTEN) (Al-Khouri *et al.*, 2005) and increases the level of phosphorylation on Ser^{473} of PKB/Akt, resulting in PKB/Akt activation. Matrix metalloproteinases (MMPs) may also play important roles in tumour invasion and metastasis (Johnsen *et al.*, 1998). The MMPs are a large family of zinc-dependent endopeptidases capable of degrading extracellular matrix components (Woessner, 1991) and the 72 kDa MMP-2 and the 92 kDa MMP-9 degrade collagens (gelatins) in the basement membrane (Murphy *et al.*, 1989), thus facilitating penetration of cancer cells through the blood vessel walls, allowing them to metastasize to other tissues or organs.

Recombinant DNA-derived VP1 (rVP1) capsid protein of the foot-and-mouth disease virus (FMDV) causes the apoptosis of cancer cells including MCF-7 (a breast carcinoma cell line), PC-3 (an androgen-independent prostate cancer cell line) and 22Rv1 (an androgen-responsive prostate cancer cell line) cells *in vitro* (Peng *et al.*, 2004). rVP1 elicited several pro-apoptotic responses, such as activation of GSK-3β and cleavage of procaspase-3, -7 and -9 (Peng *et al.*, 2004). Whether FMDV rVP1 has any anti-tumour effects *in vivo*, however, is yet to be documented. In this study, we investigated whether rVP1 induces apoptosis in human ovarian cancer cell lines. We further evaluated the anti-tumour effects of rVP1 in real-time bioluminescence-detectable orthotopic and intraperitoneal xenograft ovarian cancer models. We also investigated whether rVP1 inhibited metastasis of ovarian cancer to distal organs as well as its potential mechanism of action by examining its effects on invasive ability as well as activation or inactivation of Akt, GSK-3β, PTEN and MMPs in ovarian cancer. Our results showed that rVP1 suppressed ovarian tumour growth and metastasis *in vivo* and prolonged survival. Suppression of tumour metastasis by rVP1 may be mediated through integrins to negatively regulate Akt/MMP-2 signalling.

Methods

Cell culture and treatment

The SKOV3 human ovarian carcinoma cell line was purchased from American Tissue Culture Collection (ATCC, Manassas, VA, USA) and maintained in McCoy's 5A medium (Gibco, Carlsbad, CA, USA) containing 10% fetal bovine serum (FBS), 2 mM L-glutamine, 100 units·mL^{-1} penicillin and 100 μg·mL^{-1} streptomycin. For drug treatment experiments, cells were cultured in a 5% CO_2-humidified atmosphere at 37°C on a 96-well plate in McCoy's 5A medium with 10% FBS and used when they reached 70–90% confluency. Cisplatin, doxorubicin and rVP1 were added to the medium without serum and incubated at 37°C for 4–24 h at the concentrations indicated. Because of its photosensitivity, doxorubicin was kept away from light to prevent inactivation of doxorubicin during the course of the treatment and stored at –80°C in stock concentrations (1 mg·mL^{-1}) to minimize degradation.

Cell viability assay

Cell viability was measured by WST-1 assay according to the manufacturer's instructions. In brief, 2×10^4 cells were added to 100 μL media per well on a 96-well plate and incubated at 37°C in 5% CO_2 overnight in a humidified incubator. The cells attached to the wells were incubated in serum-free medium and treated with serial dilutions of rVP1 or doxorubicin. After incubation at 37°C in 5% CO_2 for 4–16 h to allow the drug to take effect, 10 μL WST-1 reagent was added to each well, and the plate was placed on a shaking table. After shaking at 150 rpm for 1 min, the cells were incubated at 37°C in 5% CO_2 for another 2 h to allow the WST-1 reagent to be metabolized, the proportion of surviving cells were determined by optical density (450 nm test wavelength, 690 nm reference wavelength). The percentage of surviving cells was calculated as $(OD_{treatment}/OD_{control}) \times 100\%$ and the percentage of growth inhibition was calculated as $[1 - (OD_{treatment}/OD_{control})] \times 100\%$. IC_{50} is the concentration at which the reagent yields 50% inhibition of cell viability.

Internalization of rVP1 on SKOV3 cells

Internalization study was undertaken according to a previously reported protocol (Lucie *et al.*, 2009). Briefly, SKOV3 cells were grown for 24 h on 18 mm diameter cover glasses placed in a 12-well plate overnight. rVP1 was labelled with FITC reagent (Pierce). Cells were starved for 30 min with 10 μM cycloheximide and then incubated with 1 μM rVP1 or rVP1-FITC in serum-free medium at 4°C for 30 min and at

37°C for 10 min respectively. Cells were rinsed with PBS and then fixed with 4% formaldehyde. Fluorescent images were observed at Ex/Em = 488 nm/520 nm with a confocal microscope. (Zeiss LSM 510 Meta)

Caspase activity assay

Caspase-3 activity in SKOV3 cells was measured using a caspase-3 activation assay kit (Promega, Madison, WI, USA) according to the manufacturer's instructions. In brief, SKOV3 cells were treated with 2 μM rVP1 for different times in culture medium supplemented with 10% fetal calf serum at 37°C in a 96-well plate. After treatment, cells were incubated with 100 μL caspase substrate (Caspase-Glo Reagent) for 1 h to generate luminescence. The luminescence was measured in a plate-reading luminometer (PerkinElmer Life Sciences Victor^2 1420).

DNA fragmentation assay

DNA fragmentation was measured with an ELISA kit according to the manufacturer's instructions (Roche, Mannheim, Germany). In brief, 2×10^4 cells per well in a 96-well microplate were cultured overnight. Cells were treated with a serial dilution of drugs (rVP1 or doxorubicin) for 4, 8 or 16 h in triplicate and the microplate was then centrifuged at 200× *g* for 10 min. The supernatant was removed for detection of necrotic cells and lysis buffer (200 μL·well^{-1}) was subsequently added to the cells and incubated for 10 min at 25°C. The microplate was centrifuged again at 200× *g* for 10 min and 20 μL supernatant from the medium or lysate was transferred to a streptavidin-coated microplate. Appropriate concentrations of anti-histone and anti-DNA antibodies were added and incubated for 2 h at 25°C. The microplate was washed three times with buffer at 25°C, substrate solution was then added, incubated for 15 min at 25°C, and the optical density of each well was measured (405 nm test wavelength, 490 nm reference wavelength).

Matrigel invasion assay

In vitro invasion assays were performed as previously described (Ho *et al.*, 2009). Briefly, invasion chambers containing polycarbonate filters (8 μm pore size; Corning Costar) were placed into wells. BD Matrigel matrix (50 μg per filter; BD Biosciences, Bedford, MA, USA) was hydrated with Dulbecco's modified Eagle's medium (DMEM) supplemented with 10% FBS. Cells were harvested from cultures by tapping the flask to dislodge cells; cells were then counted and seeded (5×10^4 cells in serum-free DMEM) in the upper chamber with or without rVP1 treatment, and 10% FBS-DMEM was added to the lower chamber. After incubation at 37°C for 24 h, cells that had invaded into the other side of the membrane were fixed with methanol, while non-invading cells were mechanically removed with a cotton swab. Adherent cells on the undersurface of the filter were stained with Liu's stain (Muto Pure Chemicals). The mean number of cells per chamber was calculated and the experiments were repeated three times.

Gelatin zymographic analysis

Gelatinolytic activities of MMP-2 were evaluated as described previously (Ho *et al.*, 2009). Briefly, SKOV3 cells were treated with or without rVP1 for 24 h, and culture supernatants were collected and concentrated (Centricon columns, Millipore, Bedford, MA, USA). Cells were trypsinized and counted for reference, and the supernatants were resolved on a 10% polyacrylamide gel containing 0.1% (w/v) gelatin. Gels were then washed in 2.5% TritonX-100 followed by overnight incubation at 37°C in 50 mM Tris (pH 7.5); 10 mM $CaCl_2$; 0.15 M NaCl. After incubation, gels were stained with 0.5% Coomassie blue. Proteolysis was detected as a white zone in a dark blue field and the expression bands were quantitated using Imagegauge software (Fuji).

Isolation of intraperitoneal cells

Mice were killed by instant cervical dislocation. PBS (3mL) was then injected into the peritoneum and intraperitoneal cells were retrieved (about 2 mL) using a 5 mL syringe and a 25 gauge × 1″ needle. Cells were centrifuged at 200× *g* for 5 min at 4°C and the cell pellet was collected. To remove red blood cells, 5 pellet volumes of NH_4Cl (0.144 M) and 1/2 pellet volume of NH_4HCO_3 (0.01 M) were added and incubated at 4°C for 5 min. The cell pellet was collected by centrifugation at 200× *g* for 5 min at 4°C. Cells were cultured in McCoy's 5A medium with 20% FBS in a 5% CO_2-humidified atmosphere at 37°C for 3 days before Western blot analysis, using standard Western blot techniques following resolution by SDS-PAGE on an 8–16% gradient gel (Invitrogen).

Preparation of pCMV-GFP/luciferase-lentivirus and establishment of a stable SKOV3-GL cell line

To express both green fluorescent protein (GFP) and luciferase in SKOV3 cells, we first subcloned the Bgl II restriction fragment containing a firefly luciferase gene expression cassette from pCA-CMV-Luciferase (Clontech) into the Xho I restriction site of pLKO-Gk-GFP (Taiwan National RNAi facility). Correct orientation was confirmed by the BamHI digestion. pCMV-GFP/luciferase-lentivirus was then produced by transient calcium phosphate co-transfection of shuttle plasmid (15 μg), parental construct pCMVΔR8.91 (15 μg) and VSV-G envelope plasmid pMD.G (1.5 μg) into 293T cells. Lentivirus preparations were routinely concentrated by one round of ultracentrifugation at 82 700× *g* for 2 h. Virus particles were resuspended in HBSS using 1/100 of the total original viral supernatant volume. Titres (infection units, IU) of various lentivirus preparation batches were determined using FACS analysis (FACS-Canto, Becton Dickinson, CA, USA) to measure the proportion of GFP-positive cells after infecting 1×10^5 293T cells with different amounts (0.1–5 μL) of lentiviral supernatant in the presence of 8 μg·mL^{-1} polybrene (hexadimethrine bromide, Sigma, St. Louis, MO, USA) in 96-well plates.

SKOV3-GL cells were produced by infecting SKOV3 cells with pCMV-GFP/luciferase-lentivirus. In brief, 1×10^5 SKOV3 cells were seeded into 96-well plates and cultured overnight in McCoy's 5A medium containing 10% FBS. Then cells were infected with GFP-luciferase lentivirus at 20 multiplicity of infection with 8 μg·mL^{-1} polybrene. The highest GFP-expressing cells were sorted for further passages (FACS-Aria, Becton Dickinson, CA, USA). The GFP intensity of every passage was measured by FACS analysis. Cell lysates were also harvested for validation of luciferase activity using a Minilumat LB 9506 luminometer (Berthold, Wildbach, Germany).

Luciferase activity was also confirmed by measuring the photon counts of serial cell dilutions (1~10^5) by the IVIS Imaging System (Xenogen Corp., Alameda, , CA, USA).

Detection of luciferase activity in vivo *by bioluminescence imaging*

Female BALB/cAnN-Foxn1 nude mice (National Laboratory Animal Center, Taiwan; $n = 8$ per group) were implanted with 5×10^6 SKOV3-GL cancer cells per mouse (day 0) by intraperitoneal injection. After 4 h or 6 days, mice were treated with PBS (vehicle) or 15 mg·kg^{-1} rVP1 respectively. Treatments were repeated every 2 days for 20 days. Bioluminescence was imaged weekly, starting on day 1, until untreated SKOV3-GL-bearing mice showed signs of distress (day 34). On day 34, images were also collected after removing the abdominal wall that contained ascites. For imaging of tumours *in vivo*, 150 mg·kg^{-1} D-luciferin was injected intraperitoneally, and mice were anesthetized with isoflurane and placed in a light-proof chamber. Fifteen minutes later, a photographic (gray-scale) reference image was obtained and the bioluminescent image was collected immediately thereafter. The site and magnitude of light emission were captured by optical CCD imaging using an IVIS Imaging System with the field of view height set at 25 cm. The photographic images used a 0.2 s exposure time, 8 f per stop, a binning (resolution) factor of 2, and an open filter. The bioluminescent images used exposure times ranging from 1 to 7 s, 1 f per stop, binning factor 2, and an open filter. Bioluminescence data from defined regions of interest were analysed with Living Image software (Xenogen Corp., Alameda, CA, USA) and are presented as photon counts s^{-1} cm^{-2}. Igor image analysis software (Wavemetrics, Lake Oswego, OR, USA) was also used to obtain a pseudocolour image representing bioluminescence intensity (blue, low intensity; green, medium intensity; and red, high intensity).

Immunohistochemistry

Tumours, tissues or organs were harvested and fixed in formaldehyde (10% buffered) followed by embedding in paraffin. Samples were then processed for immunostaining. Sections were cut at a thickness of 4 μm, mounted onto slides and dried on a 37°C plate for 1 h to ensure maximum adhesion. Paraffin sections were dewaxed in xylene and rehydrated in decreasing concentrations of ethanol. All sections were treated for antigen retrieval by heating in an oven for 20 min with tissue retrieval solution (DAKO, Los Angeles, CA, USA). Immunostaining of sections was performed using anti-phospho-Akt (Ser^{473}), anti-phospho-GSK-3β (Ser^{9}) and anti-Ki67 (DAKO, Los Angeles, CA, USA) rabbit polyclonal antibodies as primary antibodies. Sections were then blocked with normal goat serum for 30 min. Subsequently, sections were stained with biotinylated goat anti-rabbit antibody (1:2000; Vector Laboratories, Burlingame, CA, USA) followed by treatment with a streptavidin-biotin-peroxidase complex (ABC-Elite, Vector Laboratories, Burlingame, CA, USA). The peroxidase reaction was developed using 3′3 diaminobenzidine (Sigma Company, St. Louis, MO, USA) as a chromogen. Negative controls were stained with non-specific IgG and the appropriate horseradish peroxidase-conjugated secondary antibody. All sections were counterstained with Gill's haematoxylin. Immunostained tumour sections were examined by bright field microscopy and imaged by CCD.

Orthotopic xenograft mouse model of ovarian cancer

All animal care and experimental studies complied with the guidelines for the care and use of laboratory animals of the National Defense Medical Center, Taiwan. Ovarian cancer cells were implanted orthotopically under the ovarian bursa of 8-week-old female nude mice (BALB/cAnN-Foxn1) obtained from the National Laboratory Animal Center, Taiwan. In brief, 2.0×10^6 ovarian cancer cells (e.g. SKOV3 or stably transfected SKOV3-GL) diluted in 10 μL of PBS were injected into the bursa of the right ovary. One week after cancer cell implantation, mice were treated with rVP1 (15 mg·kg^{-1}) or PBS (vehicle) by tail vein injection three times per week for 4 weeks. At the end of the rVP1 treatment, three mice were killed for necropsy while the other mice were kept for survival studies. The percentage of survival of animals in the rVP1- and vehicle-treated groups was recorded routinely and tumour volume was determined immediately after death. Tumour volume (mm^3) was calculated using the following formula: tumour volume = 1/2 (length × width^2), in which length represents the greatest longitudinal diameter, and width the greatest transverse diameter.

Intraperitoneal xenograft mouse model of ovarian cancer

BALB/cAnN-Foxn1 female nude mice (8 weeks old) were inoculated with 5×10^6 SKOV3 or SKOV3-GL ovarian cancer cells per mouse by intraperitoneal injection (Yu *et al.*, 1993; Shaw *et al.*, 2004). Six days after cancer cell implantation, mice were treated with rVP1 (15 mg·kg^{-1}) or PBS (vehicle), and the treatments were repeated every 2 days for 60 days.

Data analysis

All statistical comparisons were made using two-tailed tests. Survival time was assessed using Kaplan–Meier curves and tested for significance using the log-rank test. Statistical evaluation was performed using SPSS 10.0 (SPSS Institute, Inc). Tissue slides were scanned and analysed by using ImageScope 9.1 software (Aperio Technologies). Isobolograms for analysis of combination treatments at different combination ratios were generated using CompuSyn 2.1 software (Chou, 2006). Differences between groups were considered statistically significant at $P < 0.05$.

Materials

Doxorubicin, cisplatin, paclitaxel, DAPI, EDTA, and RNase A were obtained from Sigma Inc. (St. Louis, MO, USA). Cell viability assay agents (WST-1), anti-histone and anti-DNA antibodies were purchased from Roche (Mannheim, Germany). Luciferin was obtained from Caliper (Madison, WI, USA). Anti-integrin β1 (MAB1965) and anti-integrin α5β1 (AB1950) antibodies for integrin blocking were obtained from Millipore (Bedford, MA, USA). Rabbit anti-phospho-PTEN (Ser^{385}), anti-PTEN, anti-poly ADP-ribose polymerase (PARP), anti-phospho-Akt (Ser^{473}), anti-Akt, anti-phospho-GSK-3β (Ser^{9}), anti-GSK-3β antibodies were obtained from Cell Signaling Technology (Beverly, MA, USA). Mouse anti-phospho-FAK

(Tyr^{397}), anti-FAK antibodies were obtained from BD Biosciences (Bedford, MA, USA). Rabbit anti-Ki67 antibody was obtained from Biocare Medical (Concord, CA, USA). MMP-2 and MMP-9 inhibitors were obtained from Calbiochem (La Jolla, CA, USA). siRNAs for integrin β1 and integrin β3 were obtained from Santa Cruz Biotechnology (St. Louis, MO, USA). The wild-type, dominant-active and dominant-negative expression plasmids of Akt were obtained from Upstate. All chemicals were of HPLC grade or higher purity. The rVP1 used in this study was the mutant form (VP1^{C187S}) (Peng *et al.*, 2004).

Results

rVP1 induces apoptosis and suppresses invasion of ovarian cancer cells in vitro

FMDV rVP1 induces apoptosis in human breast and prostate cancer cell lines such as MCF-7, PC-3 and 22Rv1, *in vitro* (Peng *et al.*, 2004). To evaluate whether rVP1 also has a cytotoxic effect on human ovarian cancer cells, we treated three human ovarian cancer cell lines (doxorubicin-resistant SKOV3, cisplatin-resistant OVCAR-3, and TOV-21G) with rVP1. Both SKOV3 and OVCAR-3 cell lines were more sensitive to rVP1 treatment than TOV-21G (IC_{50} values 0.70 ± 0.01 μM vs. 0.90 ± 0.03 μM; $P < 0.05$; Figure 1A). Comparison of rVP1, doxorubicin and cisplatin in SKOV3 cells in serum-free medium showed that rVP1 was the most effective with IC_{50} of 0.70 ± 0.01 μM, while IC_{50} of doxorubicin and cisplatin were 26.7 ± 1.05 μM and 94.3 ± 2.3 μM respectively ($P < 0.01$; Figure 1B). Addition of 10% fetal calf serum to the culture medium increased the survivability of cancer cells and shifted the IC_{50} of rVP1 from 0.70 to 4.5 μM which was still significantly lower than those of doxorubicin and cisplatin ($P < 0.05$; Figure 1B). The cytotoxic effect of rVP1 on SKOV3 cells was accompanied by DNA fragmentation, which was dependent not only on concentration but also on duration of rVP1 treatment (Figure S1A). Comparison of the effects of rVP1 with cisplatin demonstrated that rVP1 was more potent than cisplatin in causing DNA fragmentation (Figure 1C).Along with DNA fragmentation, caspase activity in SKOV3 cells was increased by rVP1 in a time-dependent manner, reaching a plateau at 6 h after rVP1 treatment (Figure S1B). rVP1 also caused cleavage of PARP (Figure S1C).

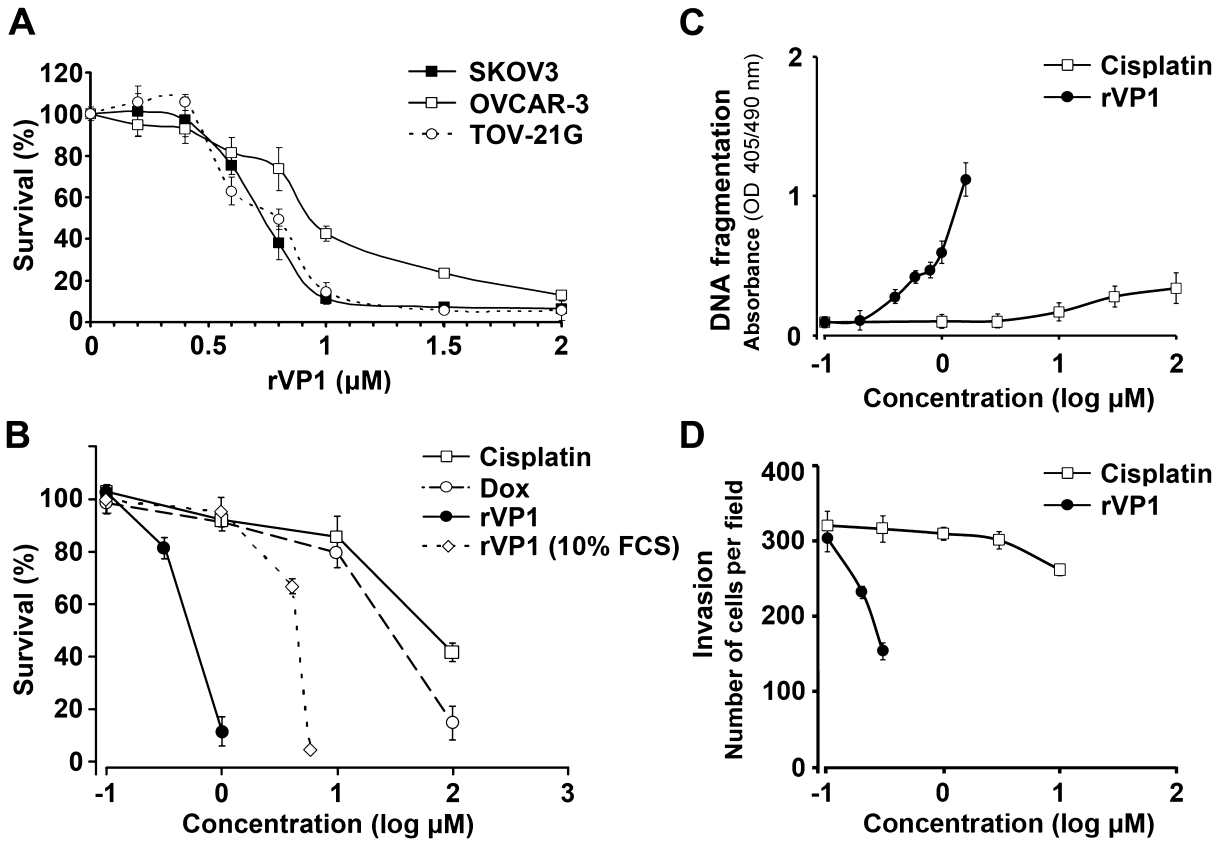

Figure 1

rVP1 decreases proliferation and invasion of ovarian cancer cells *in vitro*. Unless specified otherwise, cells were treated at 37°C for 24 h in serum-free or 10% fetal calf serum (FCS) medium with various concentrations of doxorubicin, cisplatin or rVP1 as indicated. Data represent means ± SD of three or more independent experiments as indicated. (A) rVP1 inhibits a variety of human ovarian cancer cell lines ($n = 6$). (B) Comparison of cytotoxic effects of rVP1, cisplatin and doxorubicin on SKOV3 cells *in vitro* ($n = 6$). (C) Comparison of the effects of rVP1 and cisplatin on DNA fragmentation in SKOV3 cancer cells ($n = 3$). (D) Comparison of the effects of rVP1 and cisplatin on invasive ability of SKOV3 as determined by Matrigel invasion assay ($n = 3$).

Cleaved PARP is known to increase poly (ADP-ribose) which may result in apoptosis by releasing apoptosis-inducing factor from mitochondria (Chetty *et al.*, 2010). In addition, we observed that rVP1 was more effective than cisplatin in suppressing the invasiveness of SKOV3 cells as determined by the Matrigel invasion assay (Figure 1D). Interestingly, rVP1 was able to inhibit invasion of SKOV3 cells over a dose range below its IC_{50} (e.g. 0.3 μM) that did not result in significant cell death (Figures 1A and D), suggesting that rVP1 may inhibit both survival and metastasis of ovarian cancer cells.

rVP1 inhibits survival of SKOV3 cells via dephosphorylation of Akt, GSK-3β and phosphorylation of PTEN

As rVP1 has previously been shown to induce DNA fragmentation, Akt dephosphorylation, and caspase-3 activation via integrin α5β1 in other types of cancer cells (Peng *et al.*, 2004), we investigated whether inhibition of SKOV3 cells by rVPl could be reversed by anti-integrin antibodies. Treating SKOV3 cells with 1 μM rVP1 for 24 h inhibited cell survival; this inhibition was reversed by anti-integrin β1 antibody. In comparison, treatment with 0.3 μM rVP1 for 24 h did not significantly decrease cell survival (Figure 2A). We then examined whether rVP1 could be internalized. Analysis of SKOV3 cells with FITC-labelled rVP1 showed that in the presence of protein synthesis inhibitor, cycloheximide, there was more FITC-labelled rVP1 in the cells at 37°C then those at 4°C (Figure S2), indicating that rVP1 is internalized and cycloheximide might inhibit the synthesis of protein responsible for degradation of rVP1. We subsequently extracted the lysates of SKOV3 cells that had been treated with or without rVP1 and measured the levels of signalling molecules by Western blotting with specific antibodies. When cells were treated with 1 μM rVP1 for 30 min, the levels of FAK phosphorylation at Tyr^{397}, Akt phosphorylation at Ser^{473}, and GSK-3β phosphorylation at Ser^{9} decreased, while the level of PTEN phosphorylation at Ser^{385} increased; these changes were reversed by anti-integrin β1 antibodies but not by control IgG (Figure 2B). Down-regulation of phosphorylated Akt and GSK-3β by rVP1 was also found in other cells such as OVCAR-3 and MCF-7 (Figure S3). We then examined whether overexpression of wild-type Akt or constitutively active Akt could block the inhibitory effect of rVP1. Constitutively active Akt introduced into SKOV3 cells reversed cell death caused by 1 μM rVP1, whereas wild-type Akt did not (Figure 2C).

rVP1 reduces invasive capacity of SKOV3 cells via integrin and Akt/MMP-2

Because activity of MMPs has been shown to be associated with enhanced cellular invasion, we next evaluated whether rVP1 inhibited MMPs in ovarian cancer cells. Invasiveness of SKOV3 cells, as measured by Matrigel invasion assay, was reduced by 0.3 μM rVP1, and could be reversed by anti-integrin β1 antibody but not by control IgG (Figure 3A). Reduction in the invasive capacity of SKOV3 cells upon treatment with rVP1 correlated with a reduction in MMP-2 in cancer cells as determined by gelatin zymographic analysis (Figure 3B) and Western blot (Figure S4). Inhibition of MMP-2 activity upon treatment of SKOV3 cells with rVP1 was selectively attenuated by anti-integrin β1 antibody, but not by control IgG (Figure 3B).

Because MMP-2 can be induced by Akt (Zhang *et al.*, 2009; Chetty *et al.*, 2010; Park *et al.*, 2010), we further examined whether overexpression of constitutively active Akt could reverse rVP1-mediated suppression of cell invasion. Constitutively active Akt reversed rVP1-mediated reduction of cell invasion and MMP-2 activity whereas wild-type Akt and dominant-negative Akt did not (Figure 3C and D). Collectively, these results suggest that rVP1 suppresses the invasive capacity of SKOV3 cells through integrin interaction and Akt dephosphorylation, which are associated partly, if not primarily, with reduction of MMP-2 activity.

rVP1 reduces tumour growth and metastasis of SKOV3 cells in an orthotopic xenograft mouse model

To investigate the effects of rVP1 on ovarian tumours *in vivo*, we established a SKOV3-GL cell line that stably expressed both a bioluminescent molecule (firefly luciferase) and GFP. We injected the SKOV3-GL cells into the bursa of the right ovary of orthotopic ovarian xenograft mice. One week after tumour cell implantation, the mice were separated into two groups. One group was treated with PBS buffer solution (vehicle), and the other group was treated with rVP1 ($15\ mg{\cdot}kg^{-1}$) by tail vein injection. Treatments were repeated three times per week for 4 weeks. Five weeks after tumour implantation all vehicle-treated mice exhibited tumour growth. rVP1-treated mice showed significantly less tumour growth than vehicle-treated mice as measured by bioluminescence intensity (Figure 4A). Five weeks post-inoculation vehicle-treated mice had larger tumours than those of rVP1-treated mice (Figure 4B). The progression of tumours to the liver (Figure 4C) and the inguinal lymph nodes (Figure S5) was detected in vehicle-treated mice but not in rVP1-treated mice as determined by the presence or absence of green fluorescence in these organs. The morphology and haematoxylin and eosin stained sections of livers and inguinal nodes revealed the presence of tumour cells in tissue sections from vehicle-treated mice but not from mice receiving rVP1 treatment (Figure 4C and S5). We then carried out a molecular comparison of the tumours formed in the vehicle- and rVP1-treated mice. Our results showed that levels of phosphorylated Akt, phosphorylated GSK-3β and Ki67 in tumours of rVP1-treated mice were lower than those in tumours of vehicle-treated mice. In addition, TUNEL assay revealed an increase in DNA fragmentation in tumours of rVP1-treated mice (Figure 4D). Comparison of the survival curves of rVP1-treated mice with those of vehicle-treated mice showed that rVP1 treatment significantly prolonged the survival of tumour-bearing mice (Figure 4E). Collectively, these results suggest that rVP1 effectively inhibits ovarian tumour growth and suppresses metastasis of ovarian cancer cells to the liver and inguinal lymph nodes in an orthotopic xenograft mouse model through negative Akt signalling.

rVP1 reduces ovarian tumour and metastasis in an intraperitoneal xenograft mouse model

To determine whether rVP1 is effective in treating advanced-stage ovarian cancer, we used an intraperitoneal xenograft mouse model that reproduced the conditions under which

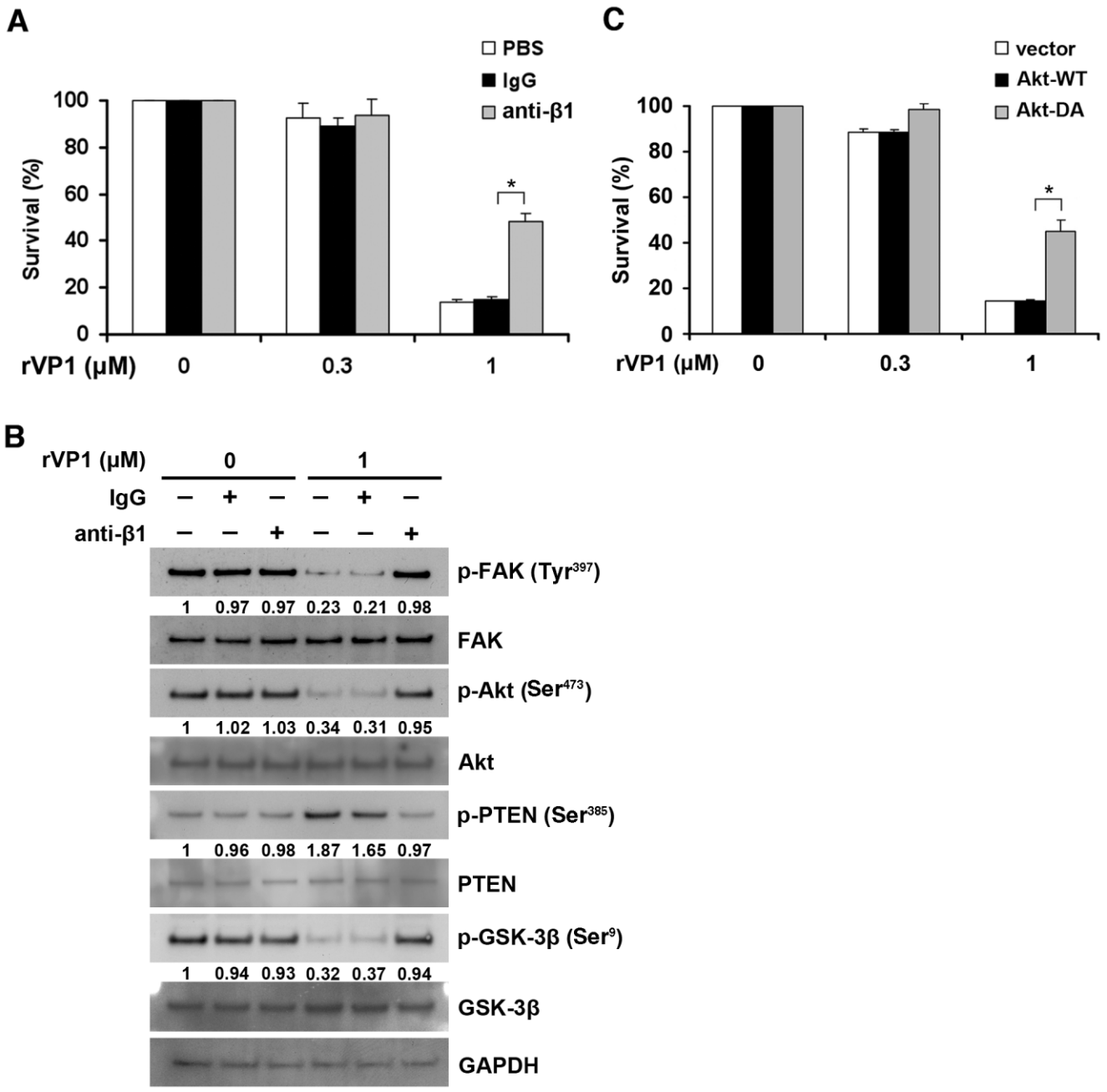

Figure 2

rVP1 inhibits cancer cell survival through integrin β1-Akt signalling. (A) SKOV3 cells were pretreated with or without anti-integrin β1 (2 μg·mL^{-1}) antibody, control IgG or PBS for 1 h then treated with 0.3 or 1 μM of rVP1 at 37°C for 24 h. Cell survival was determined by WST-1 assay. (B) SKOV3 cells were pretreated with or without control IgG or anti-integrin β1 antibody (2 μg·mL^{-1}) for 1 h followed by 1 μM of rVP1 treatment for 30 min. After incubation, lysates were analysed by Western blotting for FAK, Akt, GSK-3β, PTEN and their phosphorylated forms (p-FAK, p-Akt, p-GSK-3β and p-PTEN). Blots are representative of three independent experiments. (C) SKOV3 cells were transfected with control vector, plasmid encoding wild-type Akt (Akt-WT) or constitutively active Akt (Akt-DA) for 36 h followed by rVP1 treatment for 24 h in serum-free medium and the cell survival was determined by WST-1 assay. Data represent means ± SD of three independent experiments. *$P < 0.01$.

ovarian cancer cells accumulate within ascitic fluid in the peritoneum (Yu *et al.*, 1993; Shaw *et al.*, 2004). SKOV3-GL cells were administered by intraperitoneal injection at a dose of 5×10^6 cells per mouse (day 0) and allowed to implant for 6 days before administration of rVP1. The appropriate *in vivo* dose(s) of rVP1 was estimated by giving female nude mice increasing concentrations of rVP1 by intraperitoneal injection. Doses of 150 mg·kg^{-1} and above caused a reduction in body weight, while 15 mg·kg^{-1} of rVP1 caused little, if any, loss in body weight even after repeated administration every

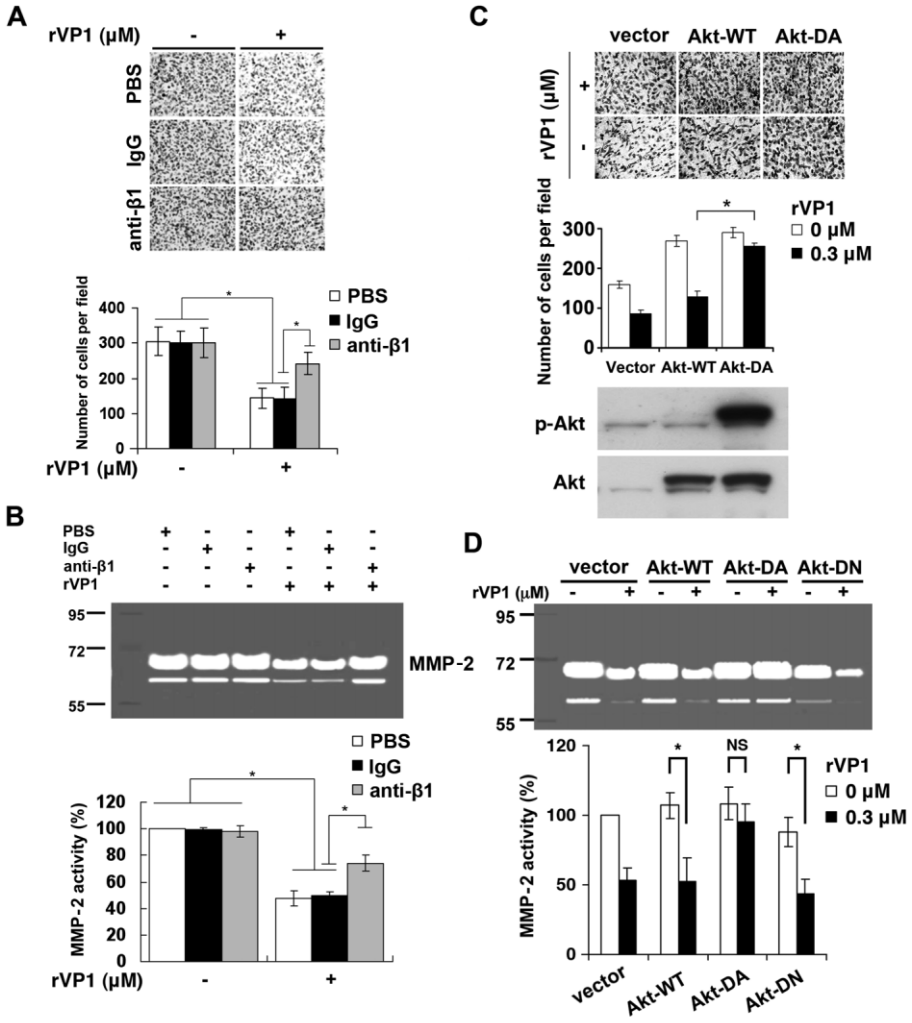

Figure 3

rVP1 suppresses invasion and MMP-2 activity of SKOV3 cells. (A) SKOV3 cells were pretreated with control IgG or anti-integrin β1 antibodies (2 μg·mL^{-1}) for 30 min followed by rVP1 treatment for 24 h in serum-free medium. The invasive ability of the cells was determined by Matrigel invasion assay. Data represent means ± SD of three independent experiments. (B) Cells were pretreated with control IgG or anti-integrin β1 antibodies (2 μg·mL^{-1}) for 30 min followed by 0.3 μM rVP1 treatment for 24 h. The MMP-2 enzyme activity in the cell-cultured medium was analysed by a gelatinolytic zymography assay. (C, D) SKOV3 cells were transfected with control vector, plasmid encoding wild-type Akt (Akt-WT), constitutively active Akt (Akt-DA) or dominant negative Akt (Akt-DN) for 36 h, followed by rVP1 treatment for 24 h in serum-free medium and the invasion and MMP-2 activity of the cells was determined. Also shown are expression levels of phosphorylated Akt or total Akt, as determined by Western blotting. Data represent means ± SD of three independent experiments *$P < 0.01$. NS, not significant.

other day for 40 days. Therefore, 15 mg·kg^{-1} was chosen as the *in vivo* treatment dosage. Six days after SKOV3-GL xenograft, rVP1 (15 mg·kg^{-1}) or vehicle was administered by intraperitoneal injection. Treatments were repeated every 2 days for 40 days. After 5 weeks, all SKOV3-GL-xenograft mice receiving vehicle treatment showed increased cancer cell growth, while the rVP1-treated, SKOV3-GL bearing mice showed mild or reduced cancer cell growth (Figure 5A). Survival analysis showed that the survival time of SKOV3-bearing mice treated with rVP1 was significantly longer than those treated with vehicle (t_{50} of 122.5 vs. 74.5 days; $P < 0.05$). Moreover, vehicle-treated mice all died within 135 days, while three out of eight (37.5%) of the rVP1-treated mice were free of cancer symptoms even after 300 days (Figure 5B).

The presence of tumours throughout the peritoneum, including ovaries, uterus, pancreas and intestines, in SKOV3-implanted mice was examined 60 days after the xenograft. Massive accumulated ascites, macronodular tumours in the gastrointestinal cavity, and tumours in the ovaries and uterus were observed. On the other hand, the surviving rVP1-treated xenograft mice, like the normal control mice, had no tumours visible on these organs (Figure S6). Haematoxylin and eosin and immunohistochemical staining of microscopic tissue sections confirmed the presence of cancer cells in the vehicle-treated but not in the control mice or some rVP1-treated mice (Figure 5C). Immunohistochemical analysis using Ki67 staining revealed that SKOV3-xenograft mice had significant numbers of Ki67-

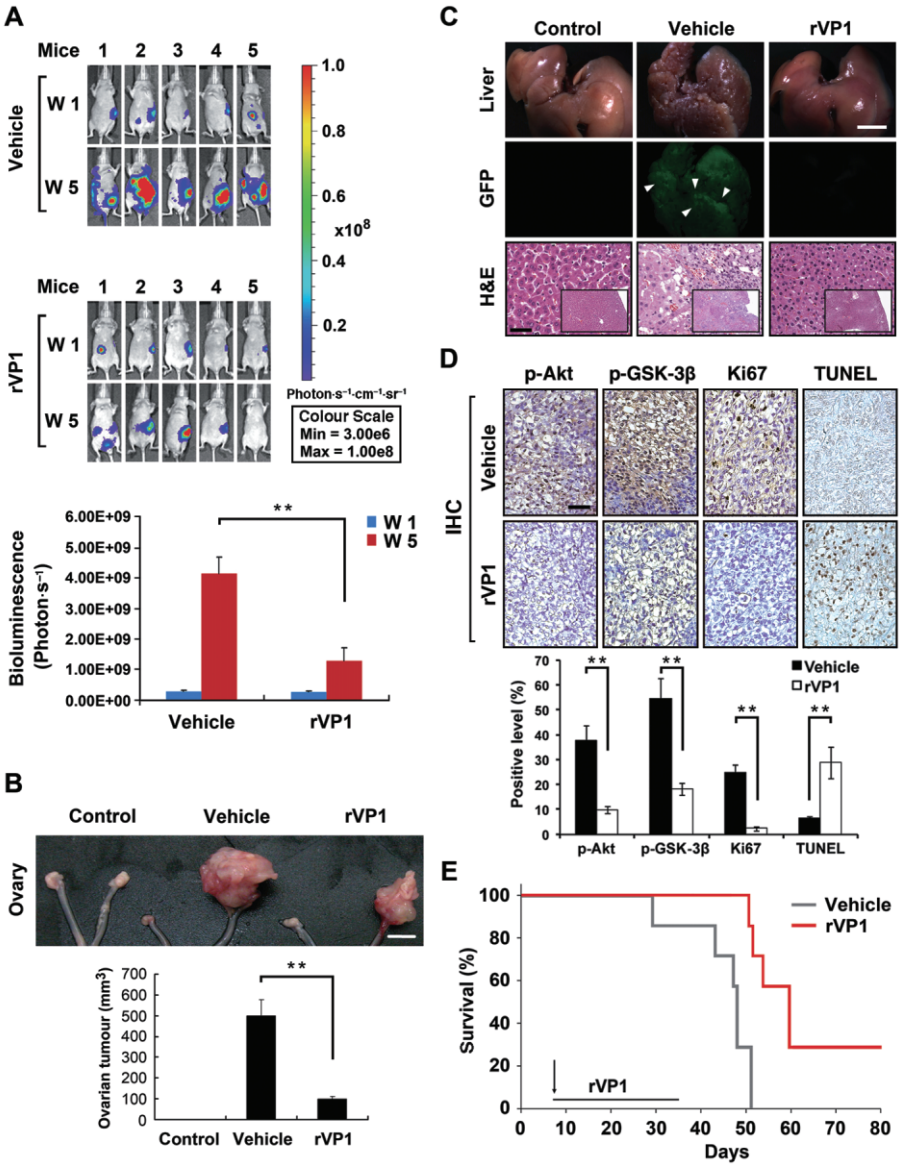

Figure 4

rVP1 attenuates SKOV3 ovarian tumour growth and metastasis in an orthotopic xenograft mouse model. SKOV3-GL-xenograft BALB/cAnN-Foxn1 female nude mice were treated with PBS (vehicle) or 15 mg·kg^{-1} rVP1 as indicated. (A) Bioluminescent images showing the presence of SKOV3-GL cells *in vivo*. Bar graphs represent photon intensity (means ± SEM). (B) Comparison of appearance and wet volume of ovaries between control mice, vehicle-treated, and rVP1-treated SKOV3-GL-xenograft mice. White scale bars, 5 mm. $^{**}P \leq 0.005$. (C) Comparison of appearance (white scale bars, 5 mm), fluorescent images and histological slides (haematoxylin and eosin [H&E]; black scale bars, 100 μm) of livers from mice from (B). (D) Ovarian tumours were harvested from mice of (B) after 5 weeks injection and processed for TUNEL and immunohistochemical (IHC) analysis with anti-phosphorylated Akt (Ser^{473}), anti-phosphorylated GSK-3β (Ser^{9}) or anti-human Ki67 antibodies. Tissue slides were scanned and analysed using ImageScope 9.1 software. Arrowheads indicate positively stained cells and data represent means ± SD of eight fixed fields within the tumour section. Black scale bars, 100 μm.$^{**}P \leq 0.005$. (E) Comparison of survival rates between the vehicle- and rVP1-treated SKOV3-xenograft mice. Vehicle treatment t_{50} = 44.5 day, rVP1 treatment t_{50} = 62.3 day; n = 7, P = 0.0047.

positive proliferating cells in ovary, uterus and liver tissue sections, while tissue sections from three rVP1-treated mice that survived to day 340 after the SKOV3 inoculation were indistinguishable from controls (Figure 5C). Taken together, these results suggest that rVP1 may be effective in inhibiting, not only the growth, but also metastasis of ovarian cancer cells to distant organs.

rVP1 suppresses invasive capacity of peritoneal adapted SKOV3 cells via integrin and Akt/MMP-2

To examine whether the peritoneal microenvironment and ascites would affect the rVP1-mediated inhibition of invasion of ovarian cancer cells, we isolated intraperitoneal ovarian

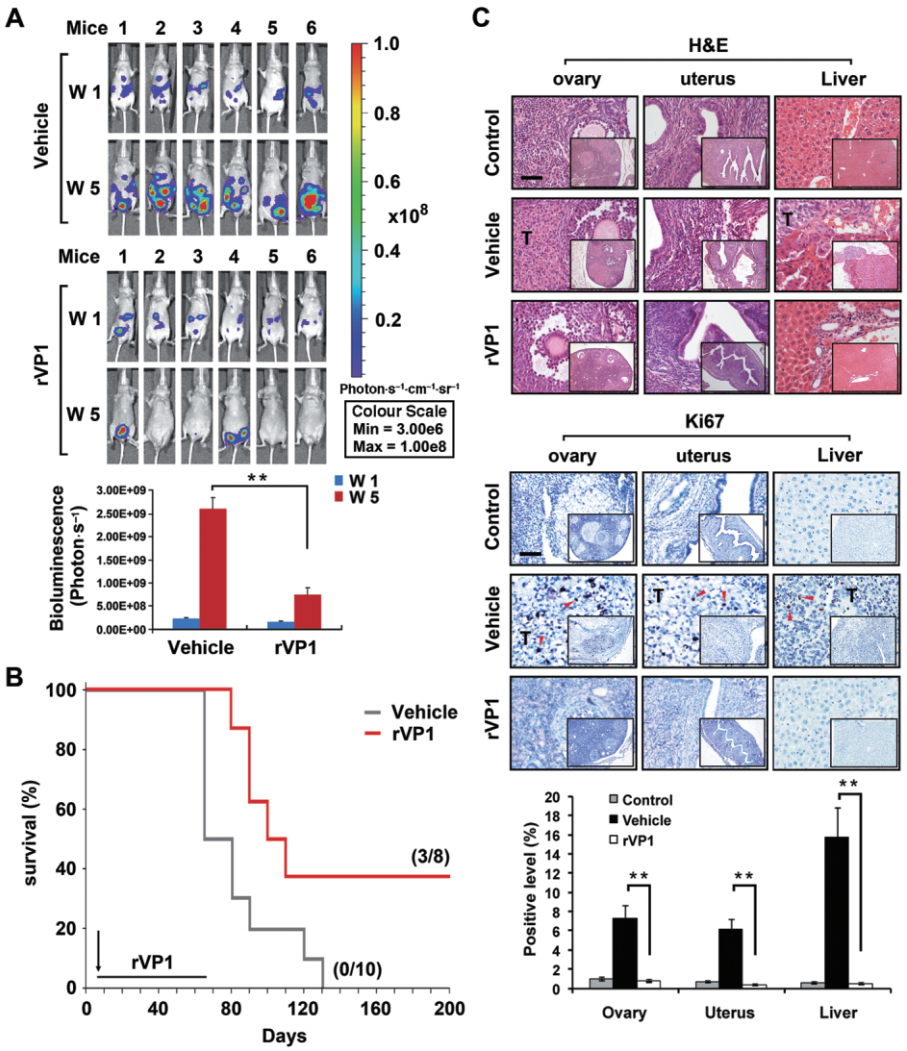

Figure 5

rVP1 attenuates tumour growth in an intraperitoneal SKOV3-xenograft mouse model. Intraperitoneal injection with vehicle or 15 mg·kg^{-1} rVP1 was started at 6 days after the SKOV3-GL inoculation. (A) Bioluminescent images showing the presence of SKOV3-GL cells *in vivo*. Bar graphs represent photon intensity (means ± SEM). (B) Comparison of survival rates between vehicle- and rVP1-treated SKOV3-xenograft mice. Vehicle treatment t_{50} = 74.5 day, n = 10; rVP1 treatment t_{50} = 122.5 day, n = 8; $P < 0.05$. (C) Ovaries, uterus and livers were collected from mice and processed for haematoxylin and eosin [H&E] staining and immunohistochemical analysis with anti-human Ki67 antibodies (indicated by red arrow). Tissue slides were scanned and analysed using ImageScope 9.1 software. Data represent means ± SD of eight fixed fields within the tumour section. Scale bars in panel C, 100 μm. $^{**}P \leq 0.005$.

cancer cells from ascites of SKOV3-bearing mice at 60 days after the implantation, referred to hereafter as SKOV3ip.1 cells. SKOV3ip.1 cells exhibited shorter doubling time than SKOV3 cells (26 h vs. 32 h). To examine whether SKOV3ip.1 cells were as sensitive as SKOV3 cells to rVP1, the inhibitory effects of rVP1 on SKOV3 and SKOV3ip.1 cells were compared. Our results showed that there was no significant difference in the effect of rVP1 on these two cell lines (Figure S7).

To assess whether rVP1 at a concentration that is not cytotoxic to cells affects the invasion and signalling pathways of SKOV3ip.1 cells, we measured the levels of signalling molecules in lysates of SKOV3ip.1 cells treated with or without 0.3 μM rVP1, *in vitro*. When SKOV3ip.1 cells were treated for 30 min with 0.3 μM rVP1, the levels of phosphorylated FAK, phosphorylated Akt, phosphorylated GSK-3β and phosphorylated PTEN were not significantly changed (Figure 6A). Prolonged treatment (24 h) with rVP1 at this concentration, however, caused a decrease in phosphorylated FAK, phosphorylated Akt and phosphorylated GSK-3β as well as an increase in the level of phosphorylated PTEN (Figure 6B). Treatment of SKOV3ip.1 cells with rVP1 in this manner decreased their invasive capacity and MMP-2 level (Figure 6C and D), but did not reduce their survival rate (Figure S7). All of the effects of rVP1 could be reversed by anti-integrin β1 antibody but not by control IgG (Figure 6A–D), suggesting that the anti-invasion effect of rVP1 was mediated via integrin β1 receptors.

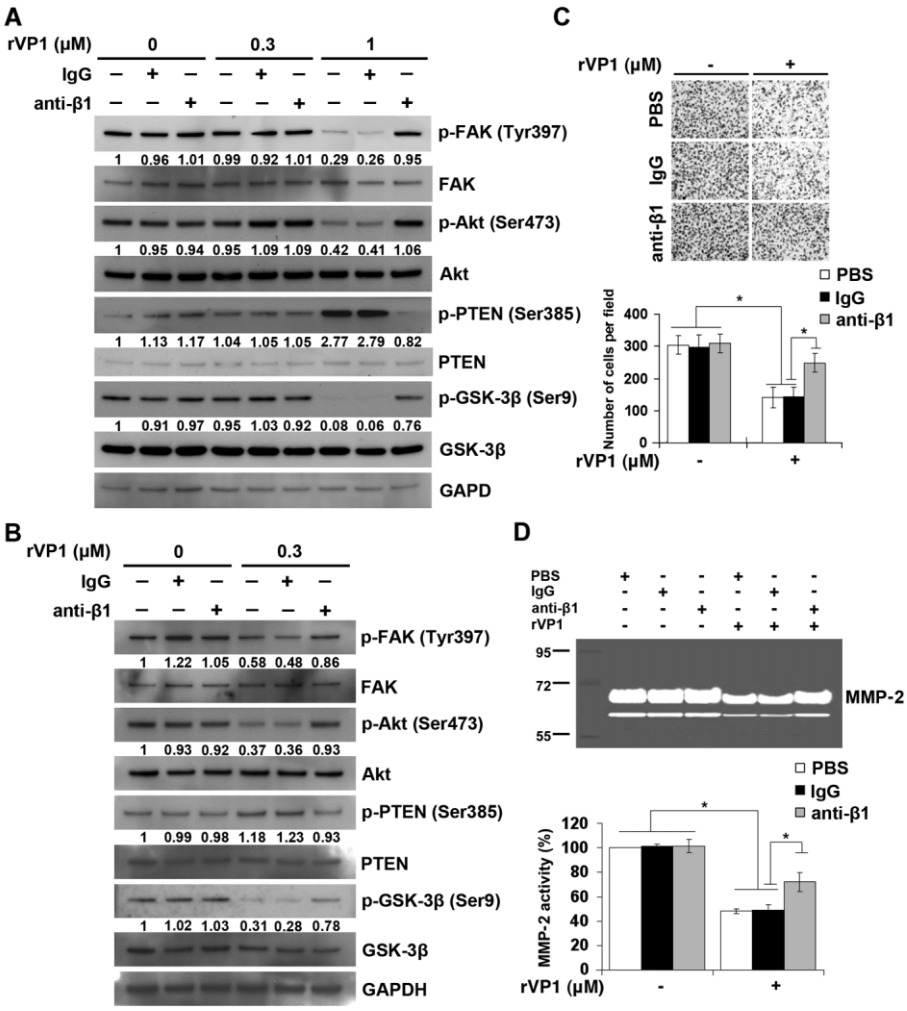

Figure 6

rVP1 suppresses invasive capacity and MMP-2 activity of SKOV3ip.1 cells through integrin β1-Akt signalling. (A) SKOV3ip.1 cells were isolated from the ascites of intraperitoneal SKOV3-xenograft mice at 60 days after the implantation. SKOV3ip.1 cells were pretreated with or without control IgG or anti-integrin β1 antibody (2 μg·mL^{-1}) for 1 h followed by 0.3 or 1 μM of rVP1 treatment for 30 min as indicated. After incubation, lysates were analysed by Western blotting for FAK, p-FAK, Akt, p-Akt, GSK-3β, p-GSK-3β, PTEN and p-PTEN. (B) SKOV3ip.1 cells were treated with or without 0.3 μM rVP1 for 24 h at 37°C in serum-free medium. After incubation, lysates were analysed by Western blotting. Blots are representative of three independent experiments. (C, D) SKOV3ip.1 cells were pretreated with control IgG or anti-integrin β1 antibodies (2 μg·mL^{-1}) for 30 min followed by 0.3 μM rVP1 treatment for 24 h in serum-free medium. The invasive capacity of the cells was determined by Matrigel invasion assay. The MMP-2 enzyme activity in the cell culture medium was analysed by a gelatinolytic zymography assay. Data represent means ± SD of three independent experiments; *P < 0.01.

Discussion and conclusions

Even after surgical removal of tumours and chemotherapy, many ovarian cancer patients develop drug resistance, suffer from cancer metastasis and die (Cannistra, 2004). Development of more effective chemotherapeutic reagents for treating metastatic ovarian cancers would therefore be beneficial. We have previously shown that rVP1 induces apoptosis in human breast and prostate cancer cell lines such as MCF-7, PC-3 and 22Rv1, *in vitro* (Peng *et al.*, 2004). In this study, we further showed that rVP1 not only induced apoptosis but also reduced the invasive capacity of human ovarian cancer SKOV3 cells and peritoneally adapted SKOV3ip.1 cells via integrin and Akt/MMP-2 (Figures 1–3 and 6). We noted, however, that treatment of rVP1 at concentrations below its IC_{50} (0.3 μM for 24 h) resulted in down-regulation of FAK phosphorylation at Tyr^{397}, Akt phosphorylation at Ser^{473}, and GSK-3β phosphorylation at Ser^{9} as well as up-regulation of PTEN phosphorylation at Ser^{385} (Figure 6A). Of note, among these four signalling molecules, after 30 min treatment with 1 μM rVP1 (pro-apoptosis condition), the increase in phosphorylated PTEN and decrease in phosphorylated GSK-3β levels were greater than those measured after treatment with 0.3 μM rVP1 for 24 h (anti-invasion condition) (Figure 6A and B). This result adds to a growing body of evidence suggesting that increase in phosphorylated PTEN and decrease in phosphorylated GSK-3β play critical roles in ovarian cancer

apoptosis (Selvendiran *et al.*, 2007). Work is currently underway to evaluate whether down-regulation of FAK phosphorylation at Tyr^{397} or Akt phosphorylation at Ser^{473} to certain threshold levels may result in MMP-2 inhibition and decreased invasion without causing apoptosis.

It should be noted that unlike rVP1, both FMDV and FMDV inactivated by binary ethylenimine inactivated, an agent known to inactivate FMDV without damaging viral proteins, did not show any apoptotic effect (Peng *et al.*, 2004). Recently, we found that FMDV or FMDV virus-like particles (Lee *et al.*, 2009) did not exhibit any apoptotic effect on SKOV3 cells (Figure S8). The apoptotic effect of rVP1 is thus most likely due to change of its conformational structure after being refolded by using our novel column process as reported for fibrillar bovine serum albumin (Huang *et al.*, 2009).

In this study, we used an orthotopic approach similar to that established by Shaw *et al.*, (2004) by injecting SKOV3 cells into the bursa of the right ovaries and using the left ovaries of BALB/cAnN-Foxn1 nude mice as controls. Even though the ovaries of orthotopic SKOV3-xenograft mice enlarged to 20 times the size of normal ovaries within 5 weeks after the injection (Figure 4B), there was little, if any, ascitic fluid in SKOV3-implanted mice and the tumours did not spread to the control ovaries, suggesting that this model mimics the early stages of ovarian cancer. Intravenous administration of rVP1 inhibited the proliferation of SKOV3 cells, decreased the occurrence of ovarian tumours, abolished metastasis of tumours to the liver and prolonged the survival of mice implanted with SKOV3- (or SKOV3-GL) cells (Figure 4). In our xenograft experiments, rVP1 was given for only a short period of time (three times a week for 4 weeks). Under these conditions, even though proliferation and metastasis of tumour cells decreased during rVP1 treatment, the cancer cells were not completely eradicated in some mice. The anti-cancer efficacy of rVP1 might be enhanced by improvement in the formulation and protocol of rVP1 administration. Collectively, these results suggest that rVP1 may be effective for treating ovarian cancer at early stages by decreasing tumour growth and inhibiting metastasis.

It must also be noted that our *in vivo* ovarian cancer experiments were undertaken in immunocompromised animals. Our preliminary results on mouse breast cancer cells in immunocompetent BALB/c mice have shown that rVP1-treated mice exhibited significantly less tumour growth and metastasis, compared with those without treatment. It will be interesting to test rVP1 for treatment of mouse and/or human ovarian cancer in an immunocompetent model.

Epithelial ovarian carcinomas progress mainly via disseminated metastasis into the peritoneal cavity and more than half of all patients are diagnosed at advanced disease stages (Auersperg *et al.*, 2001; Cannistra, 2004; Jemal *et al.*, 2009). In our intraperitoneal xenograft ovarian cancer model, we found that, similar to advanced stage ovarian cancer, SKOV3 cells accumulated in the ascitic fluid in the peritoneum as indicated by bioluminescence imaging (Figure 5A). This finding is consistent with results reported by Shaw *et al.*, (2004). However, unlike Shaw *et al.*, who reported an implantation rate of 29% ($n = 7$) for SKOV3 cells after intraperitoneal injection, we found that the implantation rate for SKOV3 was 100% ($n = 16$). This difference is likely to be due to the use of a different strain of mice (CD-1 vs. BALB/cAnN-Foxn1 nude mice). Intraperitoneal injection with rVP1 on day 6 after SKOV3 implantation rendered some SKOV3-implanted mice free of massive ascites and detectable cancer cells in the peritoneal cavity, ovary, uterus and liver (Figure 5C and S6), suggesting that rVP1 may be effective in treating disseminated ovarian cancer cells in the peritoneum during advanced stages of disease.

Intraperitoneal delivery of chemotherapy in ovarian cancer has been shown to be an effective front-line treatment. Armstrong *et al.*, (2006) undertook a randomized clinical trial in 429 patients and reported that intravenous paclitaxel plus intraperitoneal cisplatin and paclitaxel improved survival in patients with optimally debulked (no residual mass > 1 cm) stage III ovarian cancer, compared with intravenous injection of paclitaxel plus cisplatin. As the molecular weight of rVP1 (25000 Da) is 30- to 80-fold higher than that of cisplatin (MW 300 Da), doxorubicin (MW 580 Da) or paclitaxel (MW 854 Da), it will be interesting to examine whether rVP1 might be absorbed more slowly than these drugs from the peritoneal cavity and thus sustain high concentrations in the peritoneal cavity for longer to make its anti-cancer properties more effective after intraperitoneal administration.

Disintegrins are proteins often found in the venoms of various snakes of the viper family that characteristically bind with high affinity to integrins and block the interaction of integrins with tissue matrix proteins (Huang *et al.*, 1989; McLane *et al.*, 1998). Even though rVP1 contains the tripeptide RGD moiety and binds to integrins, it is distinct from disintegrins as rVP1 caused cancer cell apoptosis that was associated with dephosphorylation of phosphorylated FAK and phosphorylated Akt (Figure 2B), while some disintegrins (jarastatin and flavoridin) have been shown to increase phosphorylation of FAK (Oliva *et al.*, 2007); others, like alternagin-C, activate Akt (Cominetti *et al.*, 2004). Although some disintegrins, such as contortrostatin, exhibit anti-tumour activity, this anti-tumour effect is thought to be mainly due to anti-angiogenic effects and subsequent leakage of tumour blood vessels (Swenson *et al.*, 2005). Because rVP1 also suppressed MMPs (Figure 3B) which are known to be associated with angiogenesis (Stetler-Stevenson, 1999), it might be of interest to explore whether rVP1 has any anti-angiogenic effects, other than causing cancer cell apoptosis and suppressing metastasis.

Combination chemotherapy has been reported for inhibition of cancer proliferation and invasion (Niedzwiecki *et al.*, 2010; Spankuch and Strebhardt, 2008). It would be interesting to know whether there is any potential advantage of combination chemotherapy of rVP1 with conventional cytotoxic agents. Our preliminary results have shown a synergism between rVP1 and doxorubicin or cisplatin in the treatment of SKOV3 cells. A combination of doxorubicin or cisplatin with 0.3 μM rVP1 significantly increased cell death and decreased their IC_{50} from 26.7 to 2.7 μM or 94.3 to 5.2 μM respectively (Figure S9A and B). In contrast, no significant synergism was seen with rVP1 and paclitaxel (Figure S9C). Isobologram analyses conducted as outlined in Chou, (2006) also revealed significantly synergistic interaction, with combination indices <0.5 for cisplatin and rVP1 as well as doxorubicin and rVP1, but not for paclitaxel and rVP1. These results suggest that the action of rVP1 is comple-

mentary to that of cisplatin and doxorubicin. It might be of interest to explore whether the combination of rVP1 with doxorubicin or cisplatin has any synergistic anti-cancer effect *in vivo*.

In summary, we have shown that the rVP1 of FMDV is effective against drug-resistant human ovarian cancer cells *in vitro* and *in vivo*. rVP1 induces DNA fragmentation and apoptosis, as well as inhibition of cell metastasis, in an integrin-dependent manner that correlates with down-regulation of FAK, Akt and MMP-2 as well as activation of GSK-3β, PTEN, caspase-3 and PARP cleavage. This novel agent may be used to treat metastatic and drug-resistant ovarian cancer at both early and advanced stages.

Acknowledgements

We thank Chiao-Li Chu for her excellent assistance in protein purification, Miranda Loney (Institute of Molecular Biology, Academia Sinica, Taiwan) for English editorial assistance, and Chiao-Chun Liao, Jui-Ling Wang, Tai-An Chen and Pei-Chia Wang for technical assistance and advice. We also acknowledge grants from the National Science Council, Taiwan (NSC 96–2313-B-001–005-MY3 to S.-M.L) and Academia Sinica (to S.-M. L. and C.-M. L.).

Conflicts of interest

The authors declare no conflict of interest.

References

Al-Khouri AM, Ma Y, Togo SH, Williams S, Mustelin T (2005). Cooperative phosphorylation of the tumor suppressor phosphatase and tensin homologue (PTEN) by casein kinases and glycogen synthase kinase 3beta. J Biol Chem 280: 35195–35202.

Armstrong DK, Bundy B, Wenzel L, Huang HQ, Baergen R, Lele S *et al.* (2006). Intraperitoneal cisplatin and paclitaxel in ovarian cancer. N Engl J Med 354: 34–43.

Auersperg N, Wong AS, Choi KC, Kang SK, Leung PC (2001). Ovarian surface epithelium: biology, endocrinology, and pathology. Endocr Rev 22: 255–288.

Cannistra SA (2004). Cancer of the ovary. N Engl J Med 351: 2519–2529.

Chetty C, Lakka SS, Bhoopathi P, Rao JS (2010). MMP-2 alters VEGF expression via alphaVbeta3 integrin-mediated PI3K/AKT signaling in A549 lung cancer cells. Int J Cancer 127: 1081–1095.

Chou TC (2006). Theoretical Basis, Experimental Design, and Computerized Simulation of Synergism and Antagonism in Drug Combination Studies. Pharmacol Rev 58: 621–681.

Cominetti MR, Terruggi CH, Ramos OH, Fox JW, Mariano-Oliveira A, De Freitas MS *et al.* (2004). Alternagin-C, a disintegrin-like protein, induces vascular endothelial cell growth factor (VEGF) expression and endothelial cell proliferation in vitro. J Biol Chem 279: 18247–18255.

Dedhar S (1999). Integrins and signal transduction. Curr Opin Hematol 6: 37–43.

Delcommenne M, Tan C, Gray V, Rue L, Woodgett J, Dedhar S (1998). Phosphoinositide-3-OH kinase-dependent regulation of glycogen synthase kinase 3 and protein kinase B/AKT by the integrin-linked kinase. Proc Natl Acad Sci U S A 95: 11211–11216.

Ho MY, Leu SJ, Sun GH, Tao MH, Tang SJ, Sun KH (2009). IL-27 directly restrains lung tumorigenicity by suppressing cyclooxygenase-2-mediated activities. J Immunol 183: 6217–6226.

Huang TF, Holt JC, Kirby EP, Niewiarowski S (1989). Trigramin: primary structure and its inhibition of von Willebrand factor binding to glycoprotein IIb/IIIa complex on human platelets. Biochemistry 28: 661–666.

Huang CY, Liang CM, Chu CL, Liang SM (2009). Albumin fibrillization induces apoptosis via integrin/FAK/Akt pathway. BMC Biotechnol 9: 1–12.

Jemal A, Siegel R, Ward E, Hao Y, Xu J, Thun MJ (2009). Cancer statistics, 2009. CA Cancer J Clin 59: 225–249.

Johnsen M, Lund LR, Romer J, Almholt K, Dano K (1998). Cancer invasion and tissue remodeling: common themes in proteolytic matrix degradation. Curr Opin Cell Biol 10: 667–671.

Klauber N, Parangi S, Flynn E, Hamel E, D'Amato RJ (1997). Inhibition of angiogenesis and breast cancer in mice by the microtubule inhibitors 2-methoxyestradiol and taxol. Cancer Res 57: 81–86.

Kopfstein L, Christofori G (2006). Metastasis: cell-autonomous mechanisms versus contributions by the tumor microenvironment. Cell Mol Life Sci 63: 449–468.

Lau DH, Xue L, Young LJ, Burke PA, Cheung AT (1999). Paclitaxel (Taxol): an inhibitor of angiogenesis in a highly vascularized transgenic breast cancer. Cancer Biother Radiopharm 14: 31–36.

Lee CD, Yan YP, Liang SM, Wang TF (2009). Production of FMDV Virus-like particle by a SUMO fusion protein approach in *Escherichia coli*. J Biomed Sci 16: 69–75.

Lucie S, Elisabeth G, Stephanie F, Guy S, Amandine H, Corinne AR *et al.* (2009). Clustering and internalization of integrin $\alpha_v\beta_3$ with a tetrameric RGD-synthetic peptide. Mol Ther 17: 837–843.

Mano MS, Rosa DD, Azambuja E, Ismael G, Braga S, D'Hondt V *et al.* (2007). Current management of ovarian carcinosarcoma. Int J Gynecol Cancer 17: 316–324.

McLane MA, Marcinkiewicz C, Vijay-Kumar S, Wierzbicka-Patynowski I, Niewiarowski S (1998). Viper venom disintegrins and related molecules. Proc Soc Exp Biol Med 219: 109–119.

Murphy G, Ward R, Hembry RM, Reynolds JJ, Kuhn K, Tryggvason K (1989). Characterization of gelatinase from pig polymorphonuclear leucocytes. A metalloproteinase resembling tumour type IV collagenase. Biochem J 258: 463–472.

Niedzwiecki A, Roomi MW, Kalinovsky T, Rath M (2010). Micronutrient synergy – a new tool in effective control of metastasis and other key mechanisms of cancer. Cancer Metastasis Rev 29: 529–542.

Oliva IB, Coelho RM, Barcellos GG, Saldanha-Gama R, Wermelinger LS, Marcinkiewicz C *et al.* (2007). Effect of RGD-disintegrins on melanoma cell growth and metastasis: involvement of the actin cytoskeleton, FAK and c-Fos. Toxicon 50: 1053–1063.

Park JK, Park SH, So K, Bae IH, Yoo YD, Um HD (2010). ICAM-3 enhances the migratory and invasive potential of human non-small cell lung cancer cells by inducing MMP-2 and MMP-9 via Akt and CREB. Int J Oncol 36: 181–192.

Peng JM, Liang SM, Liang CM (2004). VP1 of foot-and-mouth disease virus induces apoptosis via the Akt signaling pathway. J Biol Chem 279: 52168–52174.

Rowinsky EK, Donehower RC (1995). Paclitaxel (taxol). N Engl J Med 332: 1004–1014.

Selvendiran K, Tong L, Vishwanath S, Bratasz A, Trigg NJ, Kutala VK *et al*. (2007). EF24 induces G2/M arrest and apoptosis in cisplatin-resistant human ovarian cancer cells by increasing PTEN expression. J Biol Chem 282: 28609–28618.

Shaw TJ, Senterman MK, Dawson K, Crane CA, Vanderhyden BC (2004). Characterization of intraperitoneal, orthotopic, and metastatic xenograft models of human ovarian cancer. Mol Ther 10: 1032–1042.

Spankuch B, Strebhardt K (2008). Combinatorial application of nucleic acid-based agents targeting protein kinases for cancer treatment. Curr Pharm Des 14: 1098–1112.

Stearns ME, Wang M (1992). Taxol blocks processes essential for prostate tumor cell (PC-3 ML) invasion and metastases. Cancer Res 52: 3776–3781.

Stetler-Stevenson WG (1999). Matrix metalloproteinases in angiogenesis: a moving target for therapeutic intervention. J Clin Invest 103: 1237–1241.

Swenson S, Costa F, Ernst W, Fujii G, Markland FS (2005). Contortrostatin, a snake venom disintegrin with anti-angiogenic and anti-tumor activity. Pathophysiol Haemost Thromb 34: 169–176.

Woessner JF Jr (1991). Matrix metalloproteinases and their inhibitors in connective tissue remodeling. FASEB J 5: 2145–2154.

Yu D, Wolf JK, Scanlon M, Price JE, Hung MC (1993). Enhanced c-erbB-2/neu expression in human ovarian cancer cells correlates with more severe malignancy that can be suppressed by E1A. Cancer Res 53: 891–898.

Zhang Z, Song T, Jin Y, Pan J, Zhang L, Wang L *et al*. (2009). Epidermal growth factor receptor regulates MT1-MMP and MMP-2 synthesis in SiHa cells via both PI3-K/AKT and MAPK/ERK pathways. Int J Gynecol Cancer 19: 998–1003.

Supporting information

Additional Supporting Information may be found in the online version of this article:

Figure S1 rVP1 causes DNA fragmentation and increases the activation of caspases and cleavage of PARP. (A) The bar graph shows that rVP1 treatment causes DNA fragmentation in SKOV3 cancer cells in a concentration- and time-dependent manner (n = 3). (B) rVP1 treatment causes caspase-3 activation in SKOV3 cancer cells. SKOV3 cells were treated with 2 μM rVP1 for different time periods at 37°C as indicated. After incubation, lysates were incubated with caspase substrate (Ac-DEVD-AFC) for 2 h. The caspase activity was measured by fluorescence at Ex/Em = 390 nm/505 nm. (C) rVP1 treatment causes cleavage of PARP. SKOV3 cells were pre-treated with or without 2 μM rVP1 for 8 h. After incubation, lysates were analysed by Western blotting using anti-PARP or anti-cleaved PARP antibodies as the primary antibodies.
Figure S2 Internalization of rVP1 in SKOV3 cells. Cells were starved for 30 min with 1 μM cycloheximide and then incubated with 1 μM rVP1 or rVP1-FITC in serum-free medium at 4°C for 30 min and at 37°C for 10 min respectively. Cells were rinsed and fixed. Fluorescent images were observed by using a single laser light at Ex/Em = 488 nm/520 nm with a confocal microscope. Bar = 50 μm.
Figure S3 rVP1 down-regulates phosphorylated Akt and GSK-3β in OVCAR-3 and MCF-7 cells. OVCAR-3 and MCF-7 cells were treated with 1 μM of rVP1 at 37°C for 30 or 60 min as indicated. After incubation, lysates were analysed by Western blotting for p-Akt and p-GSK-3β. Blots are representative of three independent experiments.
Figure S4 Quantification of MMP-2 levels by Western blot. (A) SKOV3 or (B) SKOV3ip.1 cells were pretreated with control IgG or anti-integrin β1 antibodies (2 $\mu g \cdot mL^{-1}$) for 30 min followed by 0.3 μM rVP1 treatment for 24 h. Supernatant was concentrated and analysed by Western blotting using anti-MMP-2 antibodies (*$P < 0.01$).
Figure S5 rVP1 inhibits the metastasis of tumours to the inguinal lymph nodes in orthotopic SKOV3-xenograft mice. The appearance, fluorescent images and histological slides (haematoxylin and eosin [H&E]) of inguinal nodes from control mice, vehicle-treated and rVP1-treated SKOV3-GL-xenograft mice were compared.
Figure S6 rVP1 inhibits tumour growth and metastasis of intraperitoneal SKOV3-xenograft mice. BALB/cAnN-Foxn1 female nude mice were implanted with 5×10^6 SKOV3 cancer cells *per* mouse by intraperitoneal injection. (A) Photos of vehicle- and rVP-1-treated mice 60 days post SKOV3 xenograft: the vehicle-treated mouse had massive ascites and ovaries much larger than normal due to SKOV3 tumour while the rVP1-treated mice appeared normal. (B) Necroscopy shows the presence of macronodular tumours (indicated by arrow) inside the belly of vehicle-treated SKOV3 mice and the absence of tumours in the rVP1-treated mice on 60 days post SKOV3 implantation. Photos are representative of three vehicle- and rVP1-treated mice.
Figure S7 SKOV3ip.1 cells are as sensitive as SKOV3 cells to the cytotoxic effect of rVP1. SKOV3 and SKOV3ip.1 cells were treated with various concentrations of rVP1 at 37°C for 24 h. Cell survival was determined by WST-1 assay. Data represent means ± SD of three independent experiments.
Figure S8 Comparison of the DNA fragmentation and phosphorylation of FAK and Akt in SKOV3 cells after rVP1, FMDV, or FMDV virus-like particle (VLP) treatment. (A) rVP1 but not FMDV VLP causes DNA fragmentation of SKOV3 cells. Cells were treated at 37°C for 24 h in serum-free medium with various concentrations of rVP1 or FMDV VLP as indicated. Data represent means ± SD of three independent experiments. (B) FMDV does not cause DNA fragmentation of SKOV3 cells. Cells were treated with FMDV for 24 h at 37°C in serum-free medium with serial dilutions of FMDV as indicated. $TCID_{50}$ represents the median tissue culture infective dose of FMDV O/Taiwan/97 that produces pathological change in 50% of pig cell cultures. (C) rVP1 but not FMDV VLP or FMDV decreases p-FAK and p-Akt. After incubation at 37°C for 24 h in serum-free medium with rVP1, FMDV or

FMDV VLP as indicated, cells were lysed and lysates were analysed by Western blotting. Blots are representative of three independent experiments.

Figure S9 rVP1 shows synergistic effect with doxorubicin or cisplatin but not with paclitaxel in SKOV3 cells. (A–C) The dose-dependent cytotoxic effect of doxorubicin, cisplatin or paclitaxel alone was compared with that of doxorubicin, cisplatin or paclitaxel combined with 0.3 μM rVP1 after 24 h treatment at 37°C. Cell survival was determined by WST-1 assay. IC_{50} for doxorubicin alone or combination of doxorubicin with rVP1, was 26.7 ± 1.05 μM and 2.7 ± 0.31 μM respectively. IC_{50} for cisplatin alone or combination of cisplatin with rVP1, was 94.3 ± 2.3 μM and 5.2 ± 0.67 μM respectively. IC_{50} for paclitaxel alone or combination of paclitaxel with rVP1, was 13.4 ± 0.73 μM and 12.2 ± 1.33 μM. Data represent means ± SEM. The right panel represents the normalized isobologram for combination treatments at different combination ratios visualized using CompuSyn 2.1 software. The straight line represents the additive effects of the drug combinations. Dots located below the line of additivity (left) indicate synergy, whereas, those above the line of additivity (right) indicate antagonism.

Please note: Wiley-Blackwell are not responsible for the content or functionality of any supporting materials supplied by the authors. Any queries (other than missing material) should be directed to the corresponding author for the article.